

# Triterpenoid-rich loquat leaf extract induces growth inhibition and apoptosis of pancreatic cancer cells through altering key flux ratios of glucose metabolism

Qing-Yi Lu<sup>1</sup>  · Xuemei Zhang<sup>2,3</sup> · Jieping Yang<sup>1</sup> · Vay-Liang W. Go<sup>1</sup> · Wai-Nang Lee<sup>2</sup>

Received: 22 August 2016 / Accepted: 6 February 2017 / Published online: 23 February 2017  
© Springer Science+Business Media New York 2017

## Abstract

**Introduction** Loquat leaf extract (LLE) is a mixture rich in terpenoids, and has broad biological activities including the inhibition of cancer cell growth. The exact metabolic mechanism of this growth inhibiting effect is not known.

**Objectives** We investigated the cellular metabolic effect of LLE, and ursolic acid (UA) on pancreatic cancer cells using a <sup>13</sup>C carbon tracing technology.

**Methods** MIA PaCa-2 cells were cultured in medium containing [1, 2-<sup>13</sup>C<sub>2</sub>]-glucose in the presence of either LLE (50 µg/ml), UA (50 µM), or metformin (1 mM). The mass isotopomer distribution of glucose, lactate, ribose, glutamate and palmitate in medium was determined. Based on the mass isotopomer distribution in metabolites we were able to determine individual <sup>13</sup>C enrichment ( $\sum M \times n$ ) and the minimum fraction of new synthesis (1-M0) in each metabolite. Several flux ratios of energy metabolic pathways were calculated from the mass isotopomer ratios of these metabolites.

**Results** We found that tumor viability was suppressed by LLE and UA in a dose dependent manner, and the

tumor-inhibiting effect was associated with the changes in oxidative/non-oxidative pentose (Ox/Non-ox) and pyruvate dehydrogenase/isocitrate dehydrogenase (PDH/ICDH) flux ratios resulting in decreased new syntheses of ribose and fatty acids.

**Conclusion** Metabolic homeostasis (balance of fluxes) in cancer cells is maintained through the regulation of metabolic fluxes by oncogenes and tumor-suppressor genes. Treatment of MIA PaCa-2 cells by LLE, UA and metformin likely altered key metabolic flux ratios affecting metabolic homeostasis required for energy and macromolecular production in tumor growth.

**Keywords** Loquat · Triterpenoid · MIA PaCa-2 cells · Tracer-based metabolomics · Mass isotopomer profile

## Abbreviations

UA Ursolic acid  
LLE Loquat leaf extract  
MET Metformin

**Electronic supplementary material** The online version of this article (doi:10.1007/s11306-017-1176-0) contains supplementary material, which is available to authorized users.

✉ Wai-Nang Lee  
WLee@labiomed.org

- <sup>1</sup> Department of Medicine, University of California, Los Angeles, CA, USA
- <sup>2</sup> Department of Pediatrics, Harbor-UCLA, Los Angeles Biomedical Research Institute, 1124 West Carson Street, RB1, Torrance, CA 90502, USA
- <sup>3</sup> Department of Biochemistry, Medical College of Dalian University, Dalian, China

## 1 Introduction

Loquat [*Eriobotrya japonica* (Thunb) Lindl.] is a fruit tree native to China and Japan. Loquat tree leaves have been used for the treatment of diabetes mellitus, chronic bronchitis, coughs and skin diseases in Traditional Chinese Medicine. Loquat leaf ethanol extract (LLE) is a mixture rich in terpenoids (Lu et al. 2009). Among the terpenoids present in LLE are ursolic acid (UA), oleanolic acid (OA), corosolic acid (CA) and maslinic acid (MA) (supplemental Fig. 1), which are also found in some fruits and vegetables (e.g., basil, balsam pear or bitter melon, mulberry, olive), and other medicinal plants (Jager et al. 2009). These pentacyclic

triterpenoid carboxylic acids recently have received much attention because of their potent anti-hyperglycemic and anti-diabetic actions (Alqahtani et al. 2013; Kunkel et al. 2012; Miura et al. 2012; Sheng and Sun 2011; Zeng et al. 2012). In addition, they inhibit tumor growth and induce apoptosis in several malignant cells including the pancreatic cancer cells (Li et al. 2012). UA has been shown to inhibit tumor growth and induce apoptosis in MIA PaCa-2, PANC-1 and Capan-1 pancreatic cancer cells. Its tumor growth inhibiting activity is associated with the changes in JNK and PI3K/AKT/NF- $\kappa$ B pathways (Li et al. 2012). Structurally modified synthetic oleanane triterpenes were reported to bind to mTOR (Yore et al. 2011) and are considered as multifunctional drugs for the prevention and treatment of chronic disease (Liby and Sporn 2012).

Studies of signaling pathways have contributed to our understanding of cancer metabolism (Levine and Puzio-Kuter 2010). However, the interactions between chemotherapeutic agents, which are mostly anti-metabolites (Vander Heiden 2011), and cancer signaling pathways are poorly understood. We previously reported that epigallocatechin gallate (EGCG), a phenolic compound from tea leaves, controls tumor cell growth and survival. EGCG and oxamate (an inhibitor of lactate dehydrogenase A) target aerobic glycolysis (the Warburg effect) via the suppression of lactate to pyruvate conversion thereby disrupting cellular metabolic homeostasis. Inhibition of tumor growth is the result of the disruption of flux balance throughout cellular metabolic network (Lu et al. 2015). The present study investigated how the terpenoid-rich LLE and one of its ingredient UA affect cellular metabolism in human pancreatic adenocarcinoma MIA PaCa-2 cells. The distribution of glucose carbon in MIA cells was studied using [1, 2- $^{13}\text{C}_2$ ]-D-glucose as the single precursor metabolic tracer. The effects of LLE on cell survival and glucose carbon distribution were determined, and compared with those of UA and metformin (MET). Isotope incorporations in metabolites, which reflect the contribution of glucose to energy production and substrate syntheses, were analyzed using gas chromatography/mass spectrometry and stable isotope-based dynamic metabolic profiling (SiDMAP) (Boros et al. 2002a). Our results show that the induction of growth suppression and apoptosis by LLE in MIA PaCa-2 cells may be attributed to the changes in key substrate flux ratios leading to the disruption of cellular metabolic homeostasis essential to cell growth and survival.

## 2 Materials and methods

### 2.1 Chemicals and stable glucose isotopes

UA, MET and unlabelled (natural) glucose were purchased from Sigma-Aldrich (St. Louis, MO). Stable [1,

2- $^{13}\text{C}_2$ ]-D-glucose was purchased from Isotec, Inc. (Miami, OH) with 99% isotope enrichment in carbon positions 1 and 2 of glucose. [U- $^{13}\text{C}_6$ ]-glucose and [U- $^{13}\text{C}_3$ ]-lactate were purchased from Cambridge Isotope Laboratories, Inc. (Tewksbury, MA) for use as GC recovery standards. Isotope incubation and treatment were performed as described previously (Lu et al. 2015).

### 2.2 Preparation of LLE extract

Crude leaf extract was prepared by the extraction of dried leaves growing in Southern California with 75% aqueous ethanol three times according to the literature (Chen et al. 2008; Lu et al. 2009). The yield of the LLE is approximately 3.5% by weight.

### 2.3 Cell culture and proliferation assay

MIA PaCa-2 (ATCC CRL1420) cells were purchased from American Type Culture Collection (ATCC, Manassas, VA). The cells were cultured in Dulbecco's modified Eagle's medium (DMEM) containing 10% FBS, 100 U/ml penicillin and 100  $\mu\text{g}/\text{ml}$  streptomycin. An aliquot of 100  $\mu\text{l}$  of cell suspension ( $1 \times 10^6$  cells/ml) was seeded in flat-bottomed 96-well plates and incubated in a humidified atmosphere containing 5%  $\text{CO}_2$  set at 37°C. In all experiments, cells were allowed to adhere and grow for 24 h in culture medium prior to exposure to various concentrations of crude LLE extract (0, 5, 10, 20, 50, 100, 150, 200  $\mu\text{g}/\text{ml}$ ) or UA (6.25, 12.5, 25, 50, 125 and 250  $\mu\text{M}$ ). After 24, 48 and 72 h, ApoTox-Glo Triplex Assay (Promega, Madison, MI) was performed following manufacturer's instruction. The assay assesses viability, cytotoxicity and caspase activation events within a single assay well. Triplicate wells were assayed for each condition and standard error (SE) was determined.

For tracer-based metabolomics (or SiDMAP) studies, cells (about  $1 \times 10^6$ ) were seeded in 60 mm tissue culture petri dishes, and supplied with 50% naturally labeled D-glucose and 50% [1, 2- $^{13}\text{C}_2$ ]-D-glucose which were dissolved in otherwise glucose- and sodium pyruvate-free DMEM with 10% FBS (Life Technologies, Carlsbad, CA). The glucose concentration was 450 mg/100 ml or 25.0 mM in each culture. Cells were treated with UA (50  $\mu\text{M}$ ), LLE (50  $\mu\text{g}/\text{ml}$ ) and MET (1 mM) for 48 h and then harvested for the measurement of metabolic profiling. Since MET has been reported to have anticancer property in pancreatic cancer cells, MET was chosen as a positive control. The concentration of LLE, UA and MET used was chosen based on published in vitro proliferation studies (Cantoria et al. 2014; Lu et al. 2015).

## 2.4 Immunoblot analysis

Cells were grown to about 80% confluence and reagents were added. After exposure to LLE (50, 100, 200 µg/ml) or UA (50, 100 µM) for 24 h, cells were lysed in cell lysis buffer containing 20 mM Tris-HCl, 0.5 M NaCl, 0.25% Triton X-100, 1 mM EDTA, 1 mM EGTA, 10 mM β-glycophosphate, 10 mM NaF, 300 µM Na<sub>3</sub>VO<sub>4</sub>, 1 mM benzamidine, 2 µM PMSF and 1 mM DTT. Protein concentrations were determined by a BCA protein assay kit (Thermo Scientific, Rockford, IL, USA). Proteins were separated by SDS-PAGE, transferred on to nitrocellulose membranes, blocked in 5% BSA and probed with the following primary antibodies: phospho-AMPKα (T172), AMPKα and GAPDH (Cell Signaling Technology, Boston, MA). Membranes were then incubated with horseradish peroxidase-conjugated secondary antibodies (Sigma) and visualized with SuperSignal™ West Femto Maximum Sensitivity Substrate (Thermo scientific) according to the manufacturer's recommended protocol. Band intensities are analyzed by IMAGEQUNT 5.2 software (Molecular Dynamics, Sunnyvale, CA).

## 2.5 Mass isotopomer determination by gas chromatography/mass spectrometry (GC/MS)

### 2.5.1 Glucose

For glucose assay, 50 µl of medium (after 24 h incubation) was mixed with 900 µl of methanol:water (8:1) to precipitate major proteins from the sample. [U-<sup>13</sup>C<sub>6</sub>]-glucose (50 µg) was added to each sample as recovery standard for quantitative analysis. After centrifugation, the supernatant was dried and glucose was converted to its aldonitrile pentaacetate derivative for GC/MS analysis (Paul Lee et al. 2010). Spectral peaks at m/z 328 to m/z 334 were monitored. After correcting natural <sup>13</sup>C abundance, mass isotopomer peaks (M0, M2 and M6) were used to calculate medium [1, 2-<sup>13</sup>C<sub>2</sub>]-glucose enrichment.

### 2.5.2 Lactate

Lactate from cell culture medium (50 µl) was extracted with ethyl acetate after acidification with hydrochloric acid. [U-<sup>13</sup>C<sub>3</sub>]-lactate was added before extraction to serve as recovery standard. The residue obtained after drying was treated with bis-trimethylsilyl trifluoroacetamide and trimethylchlorosilane (99:1, v/v) (Sulpelco) before GC-MS analysis as described (Jeoung et al. 2012). The ions m/z 219 to m/z 222 were monitored for isotopomer calculation. Molar enrichment of lactate with one <sup>13</sup>C carbon (m1), two

<sup>13</sup>C carbons (m2) and three <sup>13</sup>C carbons (m3) were determined. M3 isotopomer represented the recovery standard for the purpose of calculating lactate concentrations.

### 2.5.3 Glutamate

Cell pellets were homogenized in methanol:water (1:1 by volume). Cell debris was separated by centrifugation. Cell pellet was used for fatty acid analysis and supernatant for glutamate analysis. Glutamate was derivatized into its trifluoroacetamide butyl ester. For GC/MS analysis, ion clusters m/z 198 and m/z 152 representing C2-C5 and C2-C4 fragments were monitored.

### 2.5.4 Palmitate and fatty acids

Fatty acids were extracted after saponification of cell pellets in 30% KOH and 100% ethanol using petroleum ether. Fatty acids were converted to their methylated derivatives using 0.5 N methanolic-HCl prior to GC/MS analysis. Palmitate was monitored at m/z 270 to m/z 280.

### 2.5.5 RNA ribose

RNA ribose was isolated by acid hydrolysis of the cellular RNA chloroform-isopropanol fraction after Trizol purification of cell extracts. Subsequent work-up procedure was carried out to isolate 2-deoxyadenosine. Ribose and 2-deoxyribose were derivatized to their aldonitrile acetate prior to GC/MS analysis. Ion clusters around m/z 256 (carbons 1-5 of ribose, CI), m/z 217 (carbons 3-5 of ribose) and m/z 242 (carbons 1-4 of ribose EI) were monitored.

## 2.6 Data analysis and statistical methods

Mass spectral analyses were carried out by consecutive and independent automatic injections of 1 µl sample by the automatic sampler; analyses were accepted only if the standard sample deviation is less than 1% of the normalized peak intensity among repeated injections. Data download was performed by three consecutive manual peak integrations using modified (background subtracted) spectra under the overlapping isotopomer peaks of the total ion chromatogram (TIC) window displayed by the Chemstation software (Agilent, Palo Alto, CA). Mass isotopomer enrichment in metabolic intermediates is presented in molar fractions as M0, M1, M2, ... Mn, where n represents mass shift in Dalton (D) with an integer indicating the number of <sup>13</sup>C carbons replacing <sup>12</sup>C in metabolites.

<sup>13</sup>C enrichment ( $\sum M \times n$ ) and fraction of new molecules (1-M0): <sup>13</sup>C enrichment per molecule is given by  $\sum M \times n$  and <sup>13</sup>C enrichment per carbon is  $\sum M \times n / (\text{number of carbon in the molecule})$ . To calculate the contribution of glucose

carbon,  $^{13}\text{C}$  enrichment per carbon of the molecule is divided by  $^{13}\text{C}$  enrichment per carbon of glucose. Since the fraction of natural unlabeled molecule is  $M_0$ , the minimum fraction of newly synthesized molecule is  $(1-M_0)$  divided by the molar enrichment of the precursor. The “newly synthesized fraction” is a time point on the turnover curve and an arbitrary marker for turnover for the duration of incubation. The mass isotopomer distribution data can be summarized as fraction of labeled molecules,  $M_i/\sum M_i$  (where  $i \neq 0$ );  $^{13}\text{C}$  enrichment per molecule,  $\sum M \times n$  and newly synthesized fraction,  $(1-M_0)$ .

Calculation of flux ratios:  $^{13}\text{C}$  carbon tracing introduces  $^{13}\text{C}$  into various positions of a metabolite forming characteristic mass and position isotopomers. The distribution of

$^{13}\text{C}$  from  $[1, 2-^{13}\text{C}]$  glucose in various metabolites of glycolysis, pentose cycle, glucose oxidation, the tricarboxylic acid (TCA) cycle and fatty acid synthesis has been reviewed extensively (Boros et al. 2002b). Isotopomer distribution in a metabolite reflects pathways of synthesis as well as relative fluxes, and can be used to calculate a number of flux ratios which are the relative contribution of pathways to the synthesis and utilization of a metabolite. There are several key flux ratios that can be determined using  $[1, 2-^{13}\text{C}_2]$ -glucose as substrate, namely, (1) pentose cycle flux relative to glycolysis (PPC) (Lee et al. 1998); (2) oxidative to non-oxidative pentose metabolism (Ox/Non-ox) (Ramos-Montoya et al. 2006); (3) pyruvate carboxylase/pyruvate dehydrogenase (PC/PDH); (4) anaplerosis relative to TCA cycle flux (Y) (Lee et al. 1996); and (5) contribution of PDH to acetyl-CoA synthesis (Lee et al. 1995). M1 and M2 fractions in lactate were used to calculate pentose cycle flux relative to glycolysis. M1 lactate is generated from oxidative branch of the pentose cycle and M2 from glycolysis. (Lee et al. 1998). Pentose cycle flux (PPC) relative to glycolysis is given by (Lee et al. 1998):

$$\text{PPC} = (M1/M2)/[3 + (M1/M2)] \quad (1)$$

Since M1 and M3 in ribose are formed by the oxidative branch, and M2, M3 and M4 species are formed by the non-oxidative branch through transketolase/transaldolase (Lee et al. 1998), the oxidative vs non-oxidative ratio was determined by (Ramos-Montoya et al. 2006):

$$\text{Ox/Non-Ox} = (M1 + M3)/(M2 + M3 + 2 \times M4) \quad (2)$$

Lactate can enter into the TCA cycle either through pyruvate carboxylase (PC) or through pyruvate dehydrogenase (PDH). The action of PC labels C2-C3 while PDH labels carbon 4 and 5 of  $\alpha$ -ketoglutarate. PC/PDH is reflected by  $M2_{(C2-C3)}/M2_{(C4-C5)}$  of glutamate (Lee et al. 1996). Anaplerosis (Y) is determined from the M1/M2 ratio of glutamate and is given by the equation (Lee et al. 1996):

$$Y = M2/M1 - 0.5 \quad (3)$$

Acetyl-CoA enrichment and de novo lipogenesis were determined from the mass isotopomer distribution of palmitate as reported previously (Lee 1996). Since other source of acetyl-CoA is from glutamate through isocitrate dehydrogenase (ICDH) (Reitman et al. 2014), PDH/ICDH is given by the adjusted acetyl-CoA enrichment divided by 1 subtracting adjusted acetyl-CoA enrichment.

## 2.7 Statistical Analysis

Statistical analyses were performed using parametric unpaired, two-tailed (unless otherwise specified) independent sample “t” test as indicated with 95% confidence intervals.  $p < 0.05$  was considered to indicate significant differences in glucose carbon metabolism in control or treated cells. In order to reduce the chance of false discovery, the significant p value is roughly  $p < 0.01$  for four comparisons.

## 3 Results

### 3.1 Inhibition of tumor cell growth and survival

Cells were treated with increasing concentrations of LLE (0, 5, 10, 20, 50, 100, 150 and 200  $\mu\text{g/ml}$ ) for 24 (a), 48 (b) and 72 h (c) or UA (0, 6.25, 12.5, 25, 50, 125 and 250  $\mu\text{M}$ ) for 24 (d), 48 (e) and 72 h (f). The effect of LLE and UA treatment on the cell viability, cytotoxicity and apoptosis in MIA PaCa-2 cells were determined by an ApoTox-Glo Triplex Assay. Caspase activation in cell culture is an early and definitive hallmark of apoptosis. Caspase-3/7 activation and cell viability were simultaneously monitored, and the results are shown in Fig. 1. LLE and UA induced apoptosis through caspase-3/7 activation and reduced cell viability in a dose-dependent manner.

### 3.2 Glucose carbon distribution and substrate synthesis

MIA PaCa-2 cells were treated with 50  $\mu\text{M}$  (or 22.8  $\mu\text{g/ml}$ ) of UA, 50  $\mu\text{g/ml}$  of LLE or 1 mM of MET. The distribution of glucose carbons in various metabolites were traced by the  $^{13}\text{C}$  carbons from  $[1, 2-^{13}\text{C}_2]$ -glucose in culture medium. At the end of the incubation period, medium glucose concentrations were  $11.04 \pm 0.60$  mM for control,  $11.61 \pm 0.95$  mM for UA,  $11.06 \pm 0.24$  mM for LLE and  $11.88 \pm 0.34$  mM for MET. Medium lactate concentrations were  $11.18 \pm 0.25$  mM for control,  $11.65 \pm 1.01$  mM for UA,  $11.52 \pm 0.57$  mM for LLE and  $12.06 \pm 0.33$  mM for MET. Only cells treated with MET produced more lactate than the control ( $p < 0.01$ ). During the incubation, about 13–14 mM of glucose were consumed, and less than half of glucose uptake was converted to lactate by glycolysis. The incorporation of  $^{13}\text{C}$ -carbon atoms from the glucose into its

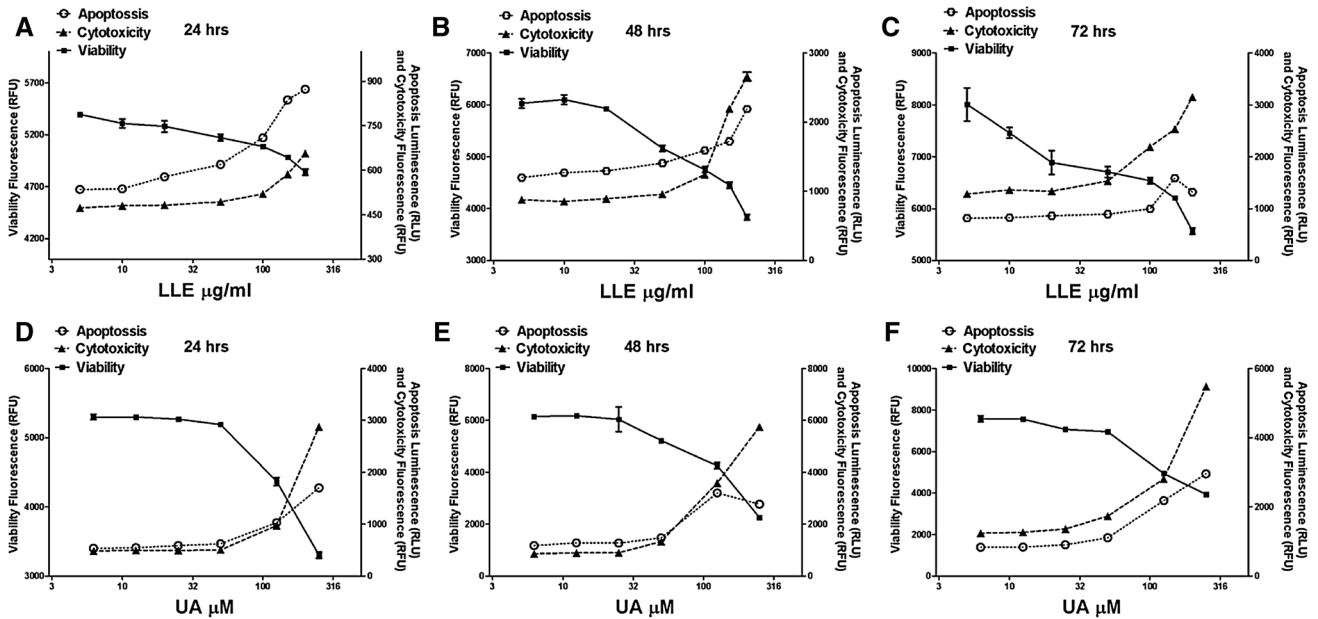


**Fig. 1** Effects of LLE and UA treatment on the viability, cytotoxicity and apoptosis of human pancreatic cancer MIA PaCa-2 cells. An ApoTox-Glo triplex assay of MIA PaCa-2 cells treated with various concentrations of LLE for 24 h (a), 48 h (b) and 72 h (c) or UA

for 24 h (d), 48 h (e) and 72 h (f) were used to determine viability and cytotoxicity with activation of caspase-3/7. Triplicate determination were averaged at each data-point. Data points represent the mean  $\pm$  SE of one of the three separate experiments

metabolites produces mass isotopomers in these metabolites. The molar fractions of mass isotopomers in lactate, ribose, glutamate and palmitate are summarized in Table 1.

The average  $^{13}\text{C}$  per carbon atom in a molecule is given by  $(\sum M \times n)/N$ , where N is the number of carbons in the molecule. For example, lactate produced by MIA cells under control condition was 0.387, and the average  $^{13}\text{C}$  per carbon atom is  $0.387/3$  or  $0.139$   $^{13}\text{C}/\text{carbon}$ , indicating that on average 13.9% of the carbon atoms in lactate was labeled with  $^{13}\text{C}$ . Similarly,  $^{13}\text{C}$  per carbon atom in the medium glucose is given by  $0.9718/6$  ( $\sum M \times n/6$ ) or  $0.1619$   $^{13}\text{C}/\text{carbon}$ . The contribution of glucose to lactate therefore is given by  $0.139/0.1619$  or 79.64%. The contributions of glucose to its metabolites by similar calculations are shown in Fig. 2a. Newly synthesized compounds are expected to be labeled with  $^{13}\text{C}$  forming  $^{13}\text{C}$  mass isotopomers. The labeled fraction (1-M0) therefore represents the fraction of molecules that are newly synthesized. Since only half of the medium glucose was labeled, the true new synthesis of a metabolite is given by (1-M0) of the metabolite divided by (1-M0) of glucose. The newly synthesized fractions are presented in Fig. 2b.

For the control group, the contribution of glucose carbon to the production of lactate, ribose, glutamate and palmitate were  $79.66 \pm 0.87\%$ ,  $97.44 \pm 1.34\%$ ,  $18.76 \pm 5.53\%$  and  $28.85 \pm 5.99\%$  respectively. Glucose contribution to lactate production in the treatment groups were not significantly different from that of the control except that of MET,

which was slightly higher than control ( $80.92 \pm 0.50\%$ ,  $p < 0.006$ ). Treatment with LLE reduced glucose incorporation into ribose, glutamate and palmitate to  $94.86 \pm 0.78\%$  ( $p < 0.013$ ),  $13.10 \pm 1.38\%$  ( $p < 0.05$  one-tail,  $p < 0.09$  two-tail), and  $15.13 \pm 4.84\%$  ( $p < 0.001$ ) respectively. MET treatment also reduced glucose incorporation into palmitate to  $22.91 \pm 3.96\%$  ( $p < 0.05$ ), but no significant effect on the ribose and glutamate. UA treatment had similar effects as LLE except that changes in glucose incorporation were not shown to be statistically different from those of no treatment.

The contribution of glucose carbon (Fig. 2a) defines two groups of metabolites: one with high contribution (80–90%) as in lactate and ribose, and the other low contribution (20–30%) as in glutamate and palmitate. These two groups are associated with high (80–90%) and low (10–20%) new fractions reflecting different turnover rates (Fig. 2b). Effects of UA, LLE and MET treatments on newly synthesized fractions or metabolite turnovers showed similar trends as shown in Fig. 2a.

### 3.3 Key metabolic flux ratios

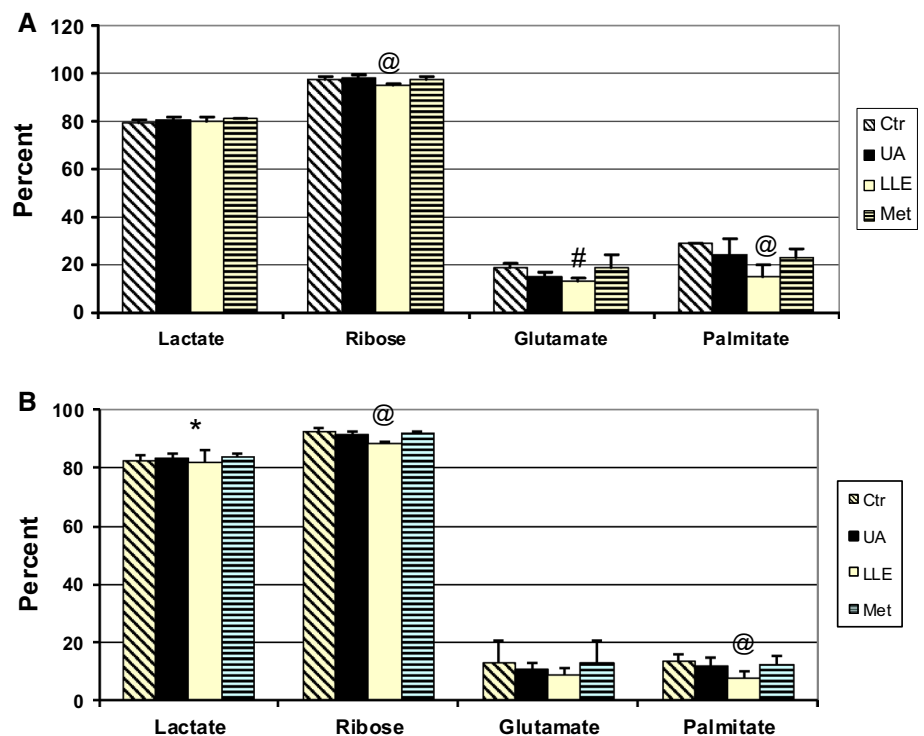
The metabolism of stable isotope ( $^{13}\text{C}$ ) labeled glucose molecules introduces  $^{13}\text{C}$  into various positions of a metabolite forming characteristic mass and position isotopomers. The isotopomer distribution in a metabolite reflects the pathways of synthesis as well as relative fluxes, and can be

**Table 1** Mass isotopomer distributions in metabolites (average  $\pm$  SD from quadruplicate samples)

		Ctr	UA	LLE	MET
Glucose	(1-M0)	0.4865 $\pm$ 0.0008	0.4860 $\pm$ 0.0007	0.4857 $\pm$ 0.0004	0.4860 $\pm$ 0.0007
	$\sum M \times n$	0.9718 $\pm$ 0.0014	0.9706 $\pm$ 0.0015	0.9704 $\pm$ 0.0007	0.9709 $\pm$ 0.0013
Lactate	M1/ $\sum M$	0.0759 $\pm$ 0.0211	0.0682 $\pm$ 0.0173	0.0637 $\pm$ 0.0405	0.0700 $\pm$ 0.0065
	M2/ $\sum M$	0.9241 $\pm$ 0.0048	0.9318 $\pm$ 0.0173	0.9363 $\pm$ 0.0405	0.9300 $\pm$ 0.0065
	(1-M0)	0.2012 $\pm$ 0.0047	0.2019 $\pm$ 0.0054	0.1982 $\pm$ 0.0093	0.2041 $\pm$ 0.0019
	$\sum M \times n$	0.3870 $\pm$ 0.0048	0.3899 $\pm$ 0.0073	0.3834 $\pm$ 0.0103	0.3938 $\pm$ 0.0026
Ribose	M1/ $\sum M$	0.4573 $\pm$ 0.0036	0.4333 $\pm$ 0.0020	0.4360 $\pm$ 0.0008	0.4434 $\pm$ 0.0020
	M2/ $\sum M$	0.3950 $\pm$ 0.0026	0.4155 $\pm$ 0.0010	0.4123 $\pm$ 0.0007	0.4054 $\pm$ 0.0011
	M3/ $\sum M$	0.0818 $\pm$ 0.0008	0.0807 $\pm$ 0.0006	0.0820 $\pm$ 0.0005	0.0836 $\pm$ 0.0004
	M4/ $\sum M$	0.0655 $\pm$ 0.0005	0.0700 $\pm$ 0.0017	0.0694 $\pm$ 0.0004	0.0673 $\pm$ 0.0018
	(1-M0)	0.4493 $\pm$ 0.0125	0.4439 $\pm$ 0.0041	0.4296 $\pm$ 0.0046	0.4452 $\pm$ 0.0030
	$\sum M \times n$	0.7884 $\pm$ 0.0115	0.7932 $\pm$ 0.0095	0.7665 $\pm$ 0.0068	0.7906 $\pm$ 0.0073
Glutamate (C2–C5)	M1/ $\sum M$	0.2739 $\pm$ 0.0066	0.2677 $\pm$ 0.0084	0.2698 $\pm$ 0.0032	0.2623 $\pm$ 0.0104
	M2/ $\sum M$	0.5568 $\pm$ 0.0664	0.5361 $\pm$ 0.0285	0.5806 $\pm$ 0.0260	0.5643 $\pm$ 0.0731
	M3/ $\sum M$	0.1692 $\pm$ 0.0606	0.1962 $\pm$ 0.0223	0.1497 $\pm$ 0.0286	0.1734 $\pm$ 0.0629
	(1-M0)	0.0638 $\pm$ 0.0167	0.0629 $\pm$ 0.0053	0.0525 $\pm$ 0.0039	0.0443 $\pm$ 0.0171
	$\sum M \times n$	0.1215 $\pm$ 0.0359	0.1220 $\pm$ 0.0108	0.0987 $\pm$ 0.0089	0.0848 $\pm$ 0.0364
	Palmitate	M2/ $\sum M$	0.5458 $\pm$ 0.0176	0.5585 $\pm$ 0.0226	0.5757 $\pm$ 0.0448
M4/ $\sum M$		0.2477 $\pm$ 0.0102	0.2334 $\pm$ 0.0060	0.1913 $\pm$ 0.0256	0.2025 $\pm$ 0.0437
	(1-M0)	0.2639 $\pm$ 0.0481	0.2265 $\pm$ 0.0631	0.1489 $\pm$ 0.0482	0.2352 $\pm$ 0.0657
	$\sum M \times n$	0.7544 $\pm$ 0.1552	0.6405 $\pm$ 0.1618	0.3834 $\pm$ 0.1252	0.5878 $\pm$ 0.126

Cells were treated with ursolic acid (UA, 50  $\mu$ M); loquat leaf extract (LLE, 50  $\mu$ g/ml) and metformin (MET, 1 mM). Ctr stands for control (no treatment).  $\sum M \times n$  is the  $^{13}$ C enrichment per molecule, (1-M0) is the fraction of labeled molecules, and  $Mn/\sum M$  is the mass isotopomer with  $n$   $^{13}$ C substitution expressed as a fraction of the labeled molecules

**Fig. 2 a** Contribution of glucose carbon to metabolite synthesis was calculated by dividing the  $^{13}$ C enrichment per carbon of the metabolite by the  $^{13}$ C enrichment per carbon of glucose. The contribution of glucose carbon to lactate, ribose, glutamate and palmitate syntheses is expressed as percent glucose carbon; **b** fraction of new synthesis was calculated by dividing (1-M0) of the metabolite by the (1-M0) of glucose. The new fraction synthesized in 48 h is expressed as percent for lactate, ribose, glutamate and palmitate. MIA PaCa-2 cells were treated with UA (50  $\mu$ M), LLE (50  $\mu$ g) or MET (1 mM) and incubated for 48 h in presence of [1, 2- $^{13}$ C<sub>2</sub>]-glucose. Columns mean, bars SD (n=4). \* $P$  < 0.05, @ $P$  < 0.01, # $P$  < 0.05 (one tail) vs untreated control



used to calculate a number of flux ratios which are important to the maintenance of metabolic homeostasis (balance of fluxes). For example, glucose can be used in both oxidative and non-oxidative branch of the pentose phosphate pathways for the nucleic acid synthesis. The ratio of oxidative/non-oxidative pentose metabolism is important for the energy balance of a cell. If glucose is used for non-oxidative pathway for ribose synthesis, then less glucose is available for NADPH production required for fatty acid synthesis. Therefore, these ratios are crucial to our understanding of cellular metabolic homeostasis. There are several key flux ratios of energy metabolism that can be determined using [1, 2-<sup>13</sup>C<sub>2</sub>]-glucose as precursor substrate. In untreated MIA cells, Ox/Non-ox ratio is  $0.8870 \pm 0.0068$ ; anaplerosis/TCA cycle flux (Y)  $1.537 \pm 0.0359$  and pyruvate dehydrogenase/isocitrate dehydrogenase contribution to acetyl-CoA (PDH/ICDH)  $1.328 \pm 0.020$ . As shown in Fig. 3 and Supplemental Table 2, treatment with UA, LLE and MET reduced these flux ratios as compared with control. While values in Y showed a trend of decreasing, changes in Ox/Non-ox and PDH/ICDH flux ratios were highly significant at  $P < 0.001$  by all treatments.

### 3.4 Inhibition of AMPK

Previous publication demonstrated that inhibition of AMPK phosphorylation induced apoptosis in MIA PaCa-2 cells (Duong et al. 2012). We performed western blotting analysis to determine the ratio of p-AMPK to T-AMPK in MIA PaCa-2 cells treated with LLE and UA at doses sufficient to induce apoptosis. Cells were exposed to LLE (50, 100 and 200  $\mu\text{g/ml}$ ) and UA (50 and 100  $\mu\text{M}$ ) for 24 h. LLE at 50  $\mu\text{g/ml}$  and UA 25  $\mu\text{M}$  showed significantly decreased AMPK phosphorylation (T172), which may be associated with the development of apoptosis (Fig. 4).

## 4 Discussion

The use of <sup>13</sup>C carbon tracing allows us to characterize metabolic phenotype in terms of glucose carbon distribution, metabolite synthesis and turnover, and metabolic flux ratios important to the maintenance of flux balance or metabolic homeostasis. Our study showed that the perturbation of these flux ratios by phytochemical treatment (Fig. 3) results in changes in the distribution of glucose carbon and

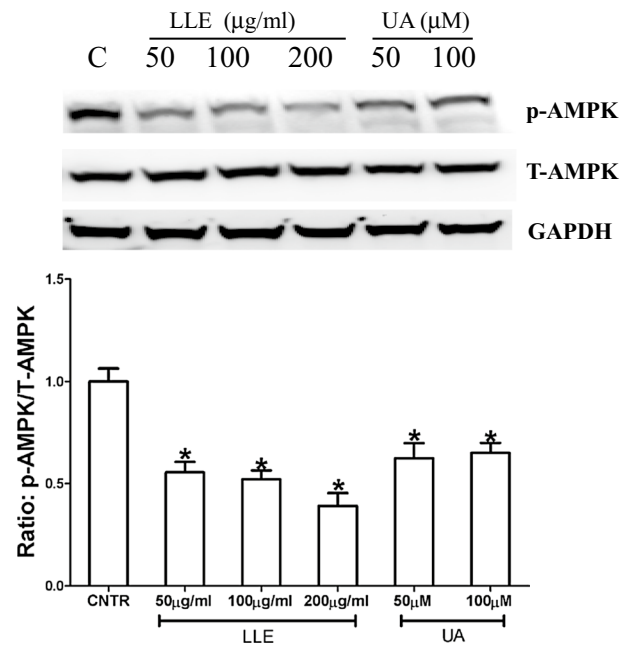


**Fig. 4** Inhibition of AMPK by UA and LLE. **a** Immunoblot analysis of p-AMPK, T-AMPK $\alpha$  and GAPDH expressions in MIA PaCa-2 cells treated with UA or LLE for 24 h at dose indicated. **b** Ratio of p-AMPK/T-AMPK $\alpha$ . Triplicate determinations were averaged at each data-point. Data represents one of the two or three separate experiments. Columns mean, bars SE (n=3). \* $P < 0.05$

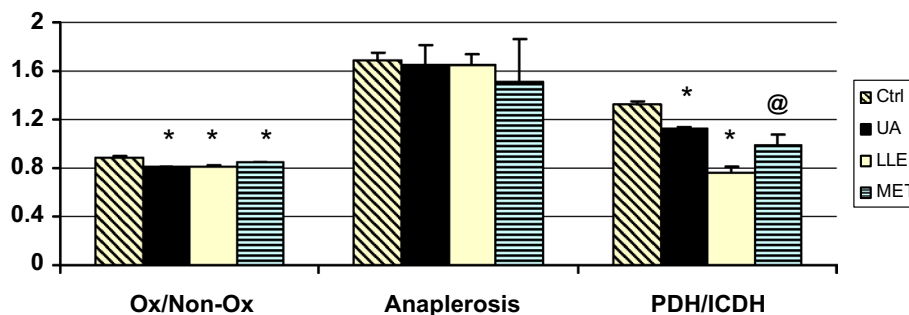


**Fig. 3** Change of key flux ratios of energy metabolism. MIA PaCa-2 cells were treated with UA (50  $\mu\text{M}$ ), LLE (50  $\mu\text{g}$ ) or MET (1 mM) and incubated for 48 h in presence of [1, 2-<sup>13</sup>C<sub>2</sub>]-glucose. Ox/Non-ox oxidative/non-oxidative pentose cycle, Anaplerosis anaplerosis/TCA

cycle flux, PDH/ICDH pyruvate dehydrogenase/isocitrate dehydrogenase contribution to acetyl-CoA. Columns mean, bars SD (n=4). \* $P < 0.05$ , @ $P < 0.03$  vs untreated control

turnover of individual metabolites leading to decreased cell survival and increased cell death.

Pentose phosphate pathways (PPP) and glycolytic pathways are intertwined, and they are mutually constrained by common metabolic intermediates (Vaitheesvaran et al. 2015). The PPP consists of an oxidative and a non-oxidative branch, and is highly active in most eukaryotes and converts glucose 6-phosphate into carbon dioxide, NADPH, and ribulose 5-phosphate for nucleic acid and amino acid syntheses. Elevated level of G6PDH together with high levels of PPP-derived metabolites were found to be associated with aggressive tumor growth in several cancer cells (Catchpole et al. 2011; Lucarelli et al. 2015; Meadows et al. 2008; Schlichtholz et al. 2005; Ying et al. 2012). In recent studies, PPP is implicated in stem cell maintenance and chemoresistance (Filosa et al. 2003; Ramos-Montoya et al. 2006). Treatment of renal carcinoma using G6PDH inhibitor 6-AN in combination with cisplatin was shown to significantly increase cell death rate, suggesting that reducing Ox/Non-ox flux ratio may be a mechanism of this targeted therapy (Lucarelli et al. 2015). In the present study, Ox/Non-ox ratio appeared to be most affected by UA, LLE and MET treatments. The change in this ratio may be the result of decreased G6PDH activity of the oxidative branch, or increased transketolase/transaldolase activity of the non-oxidative branch of the pentose phosphsate cycle. In either case the reduced cell survival was associated with fewer reducing equivalents (NADPH) for anabolic reactions such as fatty acid synthesis.

Fatty acids (FAs) are essential constituents of all biological membrane lipids and are important substrates for energy metabolism in cancer cells (Menendez and Lupu 2004). In de novo lipogenesis, acetyl-CoA is condensed with malonyl-CoA to produce palmitate, a major constituent of cell lipids. Acetyl-CoA is also a key metabolic intermediate for protein acetylation which controls key cellular processes including energy metabolism, mitosis, and autophagy (Choudhary et al. 2014; Pietrocola et al. 2015). Besides glucose and lactate, cancer cells are known to use glutamine and lipids from their environment as alternative sources of carbon for the production of acetyl-CoA and other TCA cycle intermediates (Yu et al. 2015). The contribution by glutamine and lipids from the medium reduced <sup>13</sup>C incorporation from glucose and new synthesis of glutamate and palmitate by the MIA cells. Treatment with UA, LLE or MET significantly reduced the contribution of glucose to acetyl-CoA synthesis diminishing the PDH/ICDH ratio. The change in PDH/ICDH ratio was associated with a significant decrease in de novo fatty acid synthesis essential for tumor survival and growth.

The interaction between genes and nutrient environment confers a typical metabolic phenotype to cancer cells that supports cell growth and proliferation. In cancer cells,

metabolism is regulated by a balance between oncogenes and tumor suppressor genes. For example, K-Ras, present in more than 90% of pancreatic ductal adenocarcinoma (PDAC), is known to stimulate glucose uptake and channel glucose intermediates into the hexosamine biosynthesis and PPP (Ying et al. 2012). On the other hand, P53 binds directly to G6PD and inhibits its activity, thereby suppressing the diversion of glycolytic intermediates into the PPP and reducing the production of NADPH and ribose-5-phosphate that are necessary for tumor cell growth. The mutation of P53 gene provides an uncontrolled environment for tumor cell proliferation.

Cancer metabolic phenotype can be changed by the inhibition of signaling pathways such as AMPK. AMPK is phosphorylated in response to an increase in intracellular AMP/ATP ratio. AMPK phosphorylation activates/inactivates some key metabolic enzymes, thereby inducing metabolic switch from glycolysis and anabolism to oxidative phosphorylation and catabolism. Therefore, AMPK is a sensor as well as a regulator of energy metabolism. Recent studies showed that the pharmacological inhibition of AMPK activity in some cancers results in metabolic dysregulation and apoptosis, and suggested that targeting AMPK might be potentially a useful therapeutic strategy for the treatment of some solid tumors (Jang et al. 2010; Kim et al. 2008; Zhu et al. 2010). BML-275, or compound C, is a potent and selective ATP-competitive inhibitor of AMPK that induces cell death in various types of cancers including myeloma, glioma, prostate, breast and pancreatic cancer cells (Baumann et al. 2007; Duong et al. 2012; Jin et al. 2009; Park et al. 2009; Vucicevic et al. 2009). UA and MET have been previously reported to inhibit phospho-AMPK in MIA PaCa-2 cells (Wang et al. 2015). Our data are consistent with previous report, and demonstrated that UA and LLE altered metabolic homeostasis in MIA cells that was associated with reduced phosphorylation of AMPK probably due to a change in the AMP/ATP ratio.

## 5 Conclusion

In cellular system, metabolic homeostasis is maintained by a balance of fluxes which is important for cell survival. The survival of cancer cells can be affected by metabolic inhibitors such as fatty acid synthase (FAS) inhibitor C75 (Harris et al. 2012), lactic acid dehydrogenase A inhibitor oxamate (Lu et al. 2015), kinase inhibitor imatinib (Boren et al. 2001), as well as chemicals and phytochemicals such as EGCG (Lu et al. 2015) and luteolin (Harris et al. 2012). The roles of many of these compounds including UA (a terpenoid), LLE (a mixture) and MET (a biguanide) in metabolism are poorly understood. We showed that the decrease in cell survival by the treatment of UA and LLE



was associated with significant changes in flux ratios of energy metabolism which are important to the maintenance of flux balance or metabolic homeostasis.

The mass isotopomer distribution (MID) of each metabolite in a  $^{13}\text{C}$  tracing experiment can be used to determine the balance of production and utilization (turnover) of a metabolite, and the contribution of carbon atoms from other substrates in its production. Determination of MID allows us to quantitatively measure these parameters which are characteristic of a metabolic phenotype within the context of its nutrient environment. Cellular homeostasis is impacted by changes in key flux ratios of energy metabolism, which affects  $^{13}\text{C}$  carbon distribution and substrate syntheses in metabolic intermediates. We hypothesize that the change of either signaling pathway or nutrient environment (including the treatment by drugs and phytochemicals, regardless in pure form or in mixed one) may affect cancer cell survival through the alteration of key metabolic flux ratio and the perturbation of cellular metabolic flux balance or homeostasis.

**Acknowledgements** This work was supported by the Hirshberg Foundation for Pancreatic Cancer Research and by the National Institutes of Health (P01AT003960).

#### Compliance with ethical standards

**Conflict of interest** The authors have no conflict of interest to disclose.

**Informed consent** Not applicable.

**Research involving human and animals rights** This research did not involve human or animal subjects.

## References

- Alqahtani, A., et al. (2013). The pentacyclic triterpenoids in herbal medicines and their pharmacological activities in diabetes and diabetic complications. *Current Medicinal Chemistry*, *20*, 908–931.
- Baumann, P., Mandl-Weber, S., Emmerich, B., Straka, C., & Schmidmaier, R. (2007). Inhibition of adenosine monophosphate-activated protein kinase induces apoptosis in multiple myeloma cells. *Anti-Cancer Drugs*, *18*, 405–410. doi:10.1097/CAD.0b013e32801416b6.
- Boren, J., et al. (2001). Gleevec (STI571) influences metabolic enzyme activities and glucose carbon flow toward nucleic acid and fatty acid synthesis in myeloid tumor cells. *Journal of Biological Chemistry*, *276*, 37747–37753. doi:10.1074/jbc.M105796200.
- Boros, L. G., Cascante, M., & Lee, W. N. (2002a). *Stable isotope-based dynamic metabolic profiling in disease and health: Tracer methods and applications*. Dordrecht: Kluwer Academic Publishers.
- Boros, L. G., Cascante, M., & Lee, W. N. P. (2002b). Metabolic profiling of cell growth and death in cancer: applications in drug discovery. *Drug Discovery Today*, *7*, 364–372. doi:10.1016/S1359-6446(02)02179-7.
- Cantoria, M. J., Boros, L. G., & Meuliet, E. J. (2014). Contextual inhibition of fatty acid synthesis by metformin involves glucose-derived acetyl-CoA and cholesterol in pancreatic tumor cells. *Metabolomics*, *10*, 91–104. doi:10.1007/s11306-013-0555-4.
- Catchpole, G., et al. (2011). Metabolic profiling reveals key metabolic features of renal cell carcinoma. *Journal of Cellular and Molecular Medicine*, *15*, 109–118. doi:10.1111/j.1582-4934.2009.00939.x.
- Chen, J., Li, W. L., Wu, J. L., Ren, B. R., & Zhang, H. Q. (2008). Hypoglycemic effects of a sesquiterpene glycoside isolated from leaves of loquat (*Eriobotrya japonica* (Thunb.) Lindl.). *Phytomedicine*, *15*, 98–102. doi:10.1016/j.phymed.2006.12.014.
- Choudhary, C., Weinert, B. T., Nishida, Y., Verdin, E., & Mann, M. (2014). The growing landscape of lysine acetylation links metabolism and cell signalling. *Nature Reviews. Molecular Cell Biology*, *15*, 536–550. doi:10.1038/nrm3841.
- Duong, H. Q., Hwang, J. S., Kim, H. J., Seong, Y. S., & Bae, I. (2012). BML-275, an AMPK inhibitor, induces DNA damage, G2/M arrest and apoptosis in human pancreatic cancer cells. *International Journal of Oncology*, *41*, 2227–2236. doi:10.3892/ijo.2012.1672.
- Filosa, S., et al. (2003). Failure to increase glucose consumption through the pentose-phosphate pathway results in the death of glucose-6-phosphate dehydrogenase gene-deleted mouse embryonic stem cells subjected to oxidative stress. *The Biochemical Journal*, *370*, 935–943. doi:10.1042/BJ20021614.
- Harris, D. M., Li, L., Chen, M., Lagunero, F. T., Go, V. L., & Boros, L. G. (2012). Diverse mechanisms of growth inhibition by luteolin, resveratrol, and quercetin in MIA PaCa-2 cells: a comparative glucose tracer study with the fatty acid synthase inhibitor C75. *Metabolomics*, *8*, 201–210. doi:10.1007/s11306-011-0300-9.
- Jager, S., Trojan, H., Kopp, T., Laszczyk, M. N., & Scheffler, A. (2009). Pentacyclic triterpene distribution in various plants—rich sources for a new group of multi-potent plant extracts. *Molecules*, *14*, 2016–2031. doi:10.3390/molecules14062016.
- Jang, J. H., et al. (2010). Compound C sensitizes Caki renal cancer cells to TRAIL-induced apoptosis through reactive oxygen species-mediated down-regulation of c-FLIPL and Mcl-1. *Experimental Cell Research*, *316*, 2194–2203. doi:10.1016/j.yexcr.2010.04.028.
- Jeoung, N. H., Rahimi, Y., Wu, P., Lee, W. N., & Harris, R. A. (2012). Fasting induces ketoacidosis and hypothermia in PDHK2/PDHK4-double-knockout mice. *The Biochemical Journal*, *443*, 829–839. doi:10.1042/BJ20112197.
- Jin, J., et al. (2009). AMPK inhibitor Compound C stimulates ceramide production and promotes Bax redistribution and apoptosis in MCF7 breast carcinoma cells. *Journal of Lipid Research*, *50*, 2389–2397. doi:10.1194/jlr.M900119-JLR200.
- Kim, H. S., et al. (2008). Inhibition of AMP-activated protein kinase sensitizes cancer cells to cisplatin-induced apoptosis via hyperinduction of p53. *The Journal of Biological Chemistry*, *283*, 3731–3742. doi:10.1074/jbc.M704432200.
- Kunkel, S. D., et al. (2012). Ursolic acid increases skeletal muscle and brown fat and decreases diet-induced obesity, glucose intolerance and fatty liver disease. *PLoS One*, *7*, e39332. doi:10.1371/journal.pone.0039332.
- Lee, W. N. (1996). Stable isotopes and mass isotopomer study of fatty acid and cholesterol synthesis. A review of the MIDA approach. *Advances in Experimental Medicine and Biology*, *399*, 95–114.
- Lee, W. N., Boros, L. G., Puigjaner, J., Bassilian, S., Lim, S., & Cascante, M. (1998). Mass isotopomer study of the nonoxidative pathways of the pentose cycle with [1,2- $^{13}\text{C}_2$ ] glucose. *American Journal of Physiology*, *274*, E843–E851.

- Lee, W. N., Edmond, J., Bassilian, S., & Morrow, J. W. (1996). Mass isotopomer study of glutamine oxidation and synthesis in primary culture of astrocytes. *Developmental Neuroscience*, *18*, 469–477.
- Lee, W. N. P., et al. (1995). Isotopomer study of lipogenesis in human hepatoma-cells in culture: Contribution of carbon and hydrogen atoms from glucose. *Analytical Biochemistry*, *226*, 100–112. doi:10.1006/abio.1995.1197.
- Levine, A. J., & Puzio-Kuter, A. M. (2010). The control of the metabolic switch in cancers by oncogenes and tumor suppressor genes. *Science*, *330*, 1340–1344. doi:10.1126/science.1193494.
- Li, J., Liang, X., & Yang, X. (2012). Ursolic acid inhibits growth and induces apoptosis in gemcitabine-resistant human pancreatic cancer via the JNK and PI3K/Akt/NF-kappaB pathways. *Oncology Reports*, *28*, 501–510. doi:10.3892/or.2012.1827.
- Liby, K. T., & Sporn, M. B. (2012). Synthetic oleanane triterpenoids: multifunctional drugs with a broad range of applications for prevention and treatment of chronic disease. *Pharmacological Reviews*, *64*, 972–1003. doi:10.1124/pr.111.004846.
- Lu, H., et al. (2009). Hypoglycemic and hypolipidemic effects of the total triterpene acid fraction from *Folium Eriobotryae*. *Journal of Ethnopharmacology*, *122*, 486–491. doi:10.1016/j.jep.2009.01.030.
- Lu, Q. Y., Zhang, L., Yee, J. K., Go, V. W., & Lee, W. N. (2015). Metabolic consequences of LDHA inhibition by epigallocatechin gallate and oxamate in MIA PaCa-2 pancreatic cancer cells. *Metabolomics*, *11*, 71–80. doi:10.1007/s11306-014-0672-8.
- Lucarelli, G., et al. (2015). Metabolomic profile of glycolysis and the pentose phosphate pathway identifies the central role of glucose-6-phosphate dehydrogenase in clear cell-renal cell carcinoma. *Oncotarget*, *6*, 13371–13386.
- Meadows, A. L., et al. (2008). Metabolic and morphological differences between rapidly proliferating cancerous and normal breast epithelial cells. *Biotechnology Progress*, *24*, 334–341. doi:10.1021/bp070301d.
- Menendez, J. A., & Lupu R. (2004). Fatty acid synthase-catalyzed de novo fatty acid biosynthesis: from anabolic-energy-storage pathway in normal tissues to jack-of-all-trades in cancer cells. *Arch Immunol Ther Exp* *52*, 414–426.
- Miura, T., Takagi S., & Ishida T. (2012). Management of diabetes and its complications with banaba (*Lagerstroemia speciosa* L.) and corosolic acid. *Evidence-Based Complementary and Alternative Medicine* *2012*, 871495. doi:10.1155/2012/871495.
- Park, H. U., et al. (2009). AMP-activated protein kinase promotes human prostate cancer cell growth and survival. *Molecular Cancer Therapeutics*, *8*, 733–741. doi:10.1158/1535-7163.MCT-08-0631.
- Paul Lee, W. N., Wahjudi, P. N., Xu, J., & Go, V. L. (2010). Tracer-based metabolomics: Concepts and practices. *Clinical biochemistry*, *43*, 1269–1277. doi:10.1016/j.clinbiochem.2010.07.027.
- Pietrocola, F., Galluzzi, L., Bravo-San Pedro, J. M., Madeo, F., & Kroemer, G. (2015). Acetyl coenzyme A: A central metabolite and second messenger. *Cell Metabolism*, *21*, 805–821. doi:10.1016/j.cmet.2015.05.014.
- Ramos-Montoya, A., et al. (2006). Pentose phosphate cycle oxidative and nonoxidative balance: A new vulnerable target for overcoming drug resistance in cancer. *International Journal of Cancer*, *119*, 2733–2741. doi:10.1002/ijc.22227.
- Reitman, Z. J., et al. (2014). Cancer-associated Isocitrate dehydrogenase 1 (IDH1) R132H mutation and D-2-hydroxyglutarate stimulate glutamine metabolism under hypoxia. *Journal of Biological Chemistry*, *289*, 23318–23328. doi:10.1074/jbc.M114.575183.
- Schlichtholz, B., et al. (2005). Enhanced citrate synthase activity in human pancreatic cancer. *Pancreas*, *30*, 99–104.
- Sheng, H., & Sun, H. (2011). Synthesis, biology and clinical significance of pentacyclic triterpenes: A multi-target approach to prevention and treatment of metabolic and vascular diseases. *Natural Product Reports*, *28*, 543–593. doi:10.1039/c0np00059k.
- Vaitheesvaran, B., et al. (2015). The Warburg effect: A balance of flux analysis. *Metabolomics*, *11*, 787–796. doi:10.1007/s11306-014-0760-9.
- Vander Heiden, M. G. (2011). Targeting cancer metabolism: a therapeutic window opens. *Nature Reviews: Drug Discovery*, *10*, 671–684. doi:10.1038/nrd3504.
- Vucicevic, L., et al. (2009). AMP-activated protein kinase-dependent and -independent mechanisms underlying in vitro anti-glioma action of compound C. *Biochemical Pharmacology*, *77*, 1684–1693. doi:10.1016/j.bcp.2009.03.005.
- Wang, Z., et al. (2015). Radiosensitization of metformin in pancreatic cancer cells via abrogating the G2 checkpoint and inhibiting DNA damage repair. *Cancer Letters*, *369*, 192–201. doi:10.1016/j.canlet.2015.08.015.
- Ying, H., et al. (2012). Oncogenic Kras maintains pancreatic tumors through regulation of anabolic glucose metabolism. *Cell*, *149*, 656–670. doi:10.1016/j.cell.2012.01.058.
- Yore, M. M., Kettenbach, A. N., Sporn, M. B., Gerber, S. A., & Liby, K. T. (2011). Proteomic analysis shows synthetic oleanane triterpenoid binds to mTOR. *PLoS One*, *6*, e22862. doi:10.1371/journal.pone.0022862.
- Yu, M., et al. (2015). Metabolic phenotypes in pancreatic cancer. *PLoS One* *10*, doi:10.1371/journal.pone.0115153.
- Zeng, X. Y., et al. (2012). Oleanolic acid reduces hyperglycemia beyond treatment period with Akt/FoxO1-induced suppression of hepatic gluconeogenesis in type-2 diabetic mice. *PLoS One*, *7*, e42115. doi:10.1371/journal.pone.0042115.
- Zhu, Q., et al. (2010). Inhibition of AMP-activated protein kinase pathway sensitizes human leukemia K562 cells to nontoxic concentration of doxorubicin. *Molecular and Cellular Biochemistry*, *340*, 275–281. doi:10.1007/s11010-010-0428-3.